Original Research

Abdominal MRI at 3.0 T: LAVA-Flex Compared With Conventional Fat Suppression T1-Weighted Images

Xing Hui Li, MS, Jiang Zhu, PhD, Xiao Ming Zhang, MD,* Yi Fan Ji, MS, Tian Wu Chen, MD, Xiao Hua Huang, MS, Lin Yang, MD, and Nan Lin Zeng, MS

Purpose: To study liver imaging with volume acceleration-flexible (LAVA-Flex) for abdominal magnetic resonance imaging (MRI) at 3.0 T and compare the image quality of abdominal organs between LAVA-Flex and fast spoiled gradient-recalled (FSPGR) T1-weighted imaging.

Materials and Methods: Our Institutional Review Board approval was obtained in this retrospective study. Sixty-nine subjects had both FSPGR and LAVA-Flex sequences. Two radiologists independently scored the acquisitions for image quality, fat suppression quality, and artifacts and the values obtained were compared with the Wilcoxon signed rank test. According to the signal intensity (SI) measurements, the uniformity of fat suppression, the contrast between muscle and fat and normal liver and liver lesions were compared by the paired *t*-test. The liver and spleen SI on the fat-only phase were analyzed in the fatty liver patients.

Results: Compared with FSPGR imaging, LAVA-Flex images had better and more homogenous fat suppression and lower susceptibility artifact (qualitative scores: 4.70 vs. 4.00, 4.86% vs. 7.14%, 4.60 and 4.10, respectively). The contrast between muscle and fat and between the liver and pathologic lesions was significantly improved on the LAVA-Flex sequence. The contrast value of the fatty liver and spleen was higher than that of the liver and spleen.

Conclusion: The LAVA-Flex sequence offers superior and more homogenous fat suppression of the abdomen than does the FSPGR sequence. The fat-only phase can be a simple and effective method of assessing fatty liver.

Key Words: LAVA-Flex; abdominal imaging; 3.0 T MRI; fat suppression; Dixon technique
J. Magn. Reson. Imaging 2014;40:58–66.

Sichuan Key Laboratory of Medical Imaging, Department of Radiology, Affiliated Hospital of North Sichuan Medical College, Nanchong, China.

The first two authors contributed equally to this work.

*Address reprint requests to: X.M.Z., Sichuan Key Laboratory of Medical Imaging, Department of Radiology, Affiliated Hospital of North Sichuan Medical College, Nanchong 637000, China. E-mail: cjr.zhxm@vip.163.com, zhangxm@nsmc.edu.cn

Received March 15, 2013; Accepted July 10, 2013.
DOI 10.1002/jmri.24329
View this article online at wileyonlinelibrary.com.

FAT SUPPRESSION TECHNIQUES have been routinely used in magnetic resonance imaging (MRI) of the upper abdomen (1–3). Fat-suppressed T1-weighted MRI is an important sequence, especially for differentiating between blood- and fat-containing masses, such as hemorrhagic cysts and dermoid cysts (4–6).

Various types of fat-suppression techniques have been implemented, including short-tau inversion-recovery imaging (STIR), chemical shift selective saturation (CHESS) or chemical shift selective inversion technique (CSS-IR), water-only excitation pulse approaches, and multipoint water and fat separation imaging methods such as the Dixon technique (7–11). The Dixon technique has received attention more recently because of its ability to quantify fat and robust fat separation (10–13), which permits simultaneous acquisition of in-phase, opposed-phase, water-only, and fat-only images in a single acquisition.

Liver acquisition with volume acceleration flex (LAVA-Flex) was recently introduced. The sequence is a 3D gradient dual echo imaging technique in which a second echo acquisition is added immediately after the first echo. During each repetition time, two echoes are sampled; the first read-out gradient is applied at approximately 1.3 msec, when water and fat are 180° out of phase. The second readout gradient, with opposite polarity, is then applied at 2.6 msec to acquire a second echo with the water and fat signals in phase (4). LAVA-flex then reconstructs pure water and fat images in seconds by applying a two-point Dixon method to data from in-phase and out-of-phase images (12,13). Iterative decomposition of water and fat with echo asymmetry and least-square estimation (IDEAL) is a variant of the three-point Dixon method (14,15), which is different from LAVA-flex. IDEAL also provides robust and uniform fat-separation (14) and has been used to image many body regions including the spine (16,17), musculoskeletal system (18), artery (19), and abdomen (20,21).

We conducted this study to retrospectively investigate the efficacy of LAVA-flex and compare the image quality of water-only images generated from LAVA-flex with conventional FSPGR T1-weighted CHESS fat-suppressed images obtained in patients evaluated by abdominal MRI at 3.0 T MRI.

MATERIALS AND METHODS

Patient Population

Our Institutional Review Board approved this retrospective study. Patient informed consent was waived. Our hospital medical records and radiology department databases were searched. Between October and December 2011, we chose 151 consecutive subjects with an average age of 48.9 ± 28.7 years (range: 21–67 years) who underwent abdominal MRI in a 3.0 T MR scanner (GE MR750). The following searches were used: 1) studies using both LAVA-flex and conventional fat-suppressed FSPGR T1-weighted imaging; 2) studies with cooperative patients; 3) cases with physical examinations / fatty livers / common liver local lesions, and their history, imaging characteristics, biopsy, and surgery results were used as diagnostic criteria. Eighty-two subjects were excluded, including 20 without LAVA-flex or FSPGR imaging; 9 with poor compliance; 19 with cirrhosis and ascites; 14 with bile duct diseases; 18 with pancreatitis and pancreatic lesions; and 2 with retroperitoneal tumors. Our final study population included 38 men and 31 women with an average age of 39.7 ± 23.5 years (range: 22–62 years).

MRI Technique

All examinations were conducted on a 3.0 T MR scanner with a 50 mT/m maximum gradient length and 200 T/m/s maximum slew rate (Discovery MR 750; GE Medical Systems, Milwaukee, WI) using a 16-channel body array coil with eight anterior and eight posterior elements, each arranged in a 4 × 4 configuration. All examinations were in the supine position. The sequences included FSPGR T1-weighted imaging with the CHESS technique and axial LAVA-Flex MRI as well as other conventional sequences.

FSPGR T1-weighted imaging with the CHESS technique was performed with the following parameters: repetition time (TR) / echo time (TE) = 150–180/2.1 msec; flip angle = 80°; matrix = 512 × 160–224; field of view (FOV) = 26–33 cm; section thickness = 5 mm, with 1.0 mm intersection gap, 24 sections; number of excitation (NEX) = 1; and bandwidth = 83.3 kHz with one CHESS pulse per repetition time. The acquisition time for FSPGR T1-weighted imaging was 18 seconds. This acquisition was performed with an array spatial sensitivity encoding technique (ASSET; GE Healthcare) by using a recommended acceleration factor of 2.0.

LAVA-Flex MRI was performed during one breath-hold with the following parameters: TR/TE = 4.2/2.6 msec, 1.3 msec; flip angle = 12; matrix = 320–384 × 224; section thickness = 5 mm; intersection gap = 0 mm; one acquired signal; FOV = 26–33 cm; and bandwidth = 166.7 kHz while NEX = 0.69. The acquisition time for LAVA-Flex was 17 seconds. This acquisition was performed with an array spatial sensitivity encoding technique (ASSET; GE Healthcare) by using a recommended acceleration factor of 2.0.

The FRFSE T2-weighted sequence was obtained with the following parameters: TR/TE = 10,000–12,000/90–100 msec, the TR determined by the frequency of respiration; section thickness = 5 mm; intersection gap = 0.5 mm; matrix = 256 × 192; NEX = 3; and FOV = 26–33 cm.

The SSFSE radial series slabs were obtained for MR cholangiopancreatography (MRCP) with the following parameters: TE = 1300 msec; 6 seconds between image acquisitions; section thickness = 40 mm; matrix = 384 × 224; one-half signal acquired; and FOV = 26–33 cm.

Dynamic enhanced imaging was performed with axial 3D LAVA sequencing. Scanning parameters included TR/TE = 4.0/1.9 msec; flip angle = 15°; matrix = 320 × 224; FOV = 26–33 cm; section thickness = 4–6 mm; and NEX = 0.75. Gadolinium chelate (Magnevist, Schering Guangzhou, China) was administered intravenously (0.2 mmol/L per kg of body weight) at approximately 3.5 mL/s using a double tube high-pressure injector (Spectris MR Injection System, Medrad, Pittsburgh, PA) and was followed by a 20 mL saline solution flush at the same speed. With the patient holding his/her breath, two arterial phase images were achieved in 19 seconds. From the beginning of the injection, two portal vein phase images in 60 seconds and one equilibrium phase images in 180 seconds were obtained (22).

MRI Analysis

The original MRI data were loaded onto a workstation (Advantage Workstation 4.2; GE Healthcare).

Qualitative Image Analysis

The FSPGR T1-weighted images and LAVA-Flex water-only images were evaluated independently by two radiologists (with 5 and 6 years of experience in interpreting abdominal MR images). Because the appearances of the images generated with the different sequences were obvious, the radiologists could not be blinded to the type of acquisition; however, the two radiologists were not aware of the endpoints of the study. The two readers compared the two sequences to evaluate the image quality, fat suppression quality, susceptibility artifacts, and motion artifacts (4,15). They graded the image quality using a five-point scale (23) on which 1 point indicated unacceptable quality, 2 points indicated poor quality, 3 points indicated fair quality, 4 points indicated good quality, and 5 points indicated excellent quality. The image quality of the liver lesions detected was rated with a similar five-point scale (4). All of the scores of image quality were negotiated by the two radiologists.

Quantitative Image Analysis

Uniformity of Fat Suppression

Region-of-interest (ROI) analyses of the FSPGR T1-weighted images and LAVA-Flex water-only images were performed by one investigator (with 3 years of experience in interpreting abdominal MR images) at a GE Advantage Workstation 4.2 to assess the uniformity of fat suppression. A circular 150 mm^2 ROI was placed in the superficial fat in four locations (one in each quadrant of the image) on individual sections (4). This process was repeated at three levels—the liver dome, the porta, and the renal hilum. Within a single imaging sequence, 12 measurements of the signal intensity (SI) with each sequence for each patient were obtained. Then, the percentage of the standard deviation (SD) of these measurements was calculated to yield a quantitative measurement of the uniformity of fat suppression in each acquisition for each patient (4). The percentage SD was calculated with the following equation: the SD of the ROI, divided by the mean value of the signal intensity ROI.

Contrast Between Muscle and Fat

The measurements of mean SI of the FSPGR T1-weighted images and LAVA-Flex water-only images were evaluated by placing an identical ROI over the erector spinae and adjacent superficial fat. This process was repeated at three levels, and the mean signal intensity value was acquired for each tissue. The contrast between the muscle and fat (C_{MF}) was then calculated with the following equation: $C_{MF} = (SI_M\text{-}SI_F) / SI_M$, where SI_M is the mean signal intensity in the erector spinae and SI_F is the mean signal intensity in fat (4,15).

Contrast Between Liver and Liver Lesions

We calculated the ratio for the contrast between normal liver and liver lesions by placing a comparably sized circular ROI over the most homogeneous part of each lesion and on the right liver lobe on two sequences, avoiding regional artifacts. This process was repeated three times, and the mean signal intensities of the normal liver and liver lesions were calculated. The contrast between the normal liver and liver lesions (C_{LLL}) was calculated with the formula: $C_{LLL} = (SI_L\text{-}SI_{LL}) / SI_L$, where SI_L is the mean signal intensity in the normal liver and SI_{LL} is the mean signal intensity in the liver lesion (4,15). When multiple hepatic lesions were found, we considered the lesion with the larger diameter.

Contrast Between Fatty Liver and Spleen on the Fat-Phase Imaging

The measurements of the mean SI of the FSPGR T1-weighted images and LAVA-Flex fat-only images were evaluated by placing three identical ROIs over the normal liver, spleen, and fatty liver (local/diffuse). The contrasts between the liver and spleen (C_{LS}) and fatty liver and spleen (C_{FLS}) were calculated separately using the formula $C_{LS} = (SI_L\text{-}SI_S) / SI_L$, $C_{FLS} = (SI_{FL} - SI_S) / SI_{FL}$, where SI_L, SI_S, are SI_{FL} the mean signal intensities in the normal liver, spleen, and liver fat, respectively (4,15).

Statistical Analysis

For the qualitative five-point scale evaluations, the Wilcoxon signed rank test was used to compare differences between the evaluations made with the FSPGR T1-weighted images using the CHESS technique and those with the LAVA-Flex water-only images.

For quantitative analysis, we used the paired *t*-test to compare the differences in all of the parameters (mean SD of the fat SI for 12 ROIs, the contrast between the muscle and fat, and the contrast between the normal liver and pathologic lesions) between the FSPGR T1-weighted imaging and LAVA-Flex water-only imaging. The differences in the liver and spleen SI in both the normal liver and the fatty liver patients with the fat-only phase were compared using the paired *t*-test.

The data analysis was performed using SPSS for Windows (v. 13.0, Chicago, IL). $P \leq 0.05$ was considered significant.

Table 1
Comparison of the Five-Point-Scale Qualitative Scores Between the FSPGR T1-Weighted and LAVA-Flex Water-Only Images

Parameter	LAVA-Flex water-only	FSPGR T1-weighted	*P* value
Image quality			
Overall	4.03(0.65)	3.92(0.69)	0.491
Liver	4.06(0.63)	4.00(0.72)	0.486
Pancreas	4.03(0.61)	3.94(0.67)	0.402
Spleen	4.00(0.59)	3.97(0.61)	0.691
Fat suppression quality	4.70(0.50)	4.00(0.80)	0.001
Susceptibility artifacts	4.60(0.50)	4.10(0.80)	0.009
Motion artifacts	4.5(0.5)	4.2(0.8)	0.070

The data are the mean image quality (standard deviation) based on the data obtained in 69 patients.
Scores are based on the data obtained from 39 liver lesion patients.

RESULTS

Qualitative Assessment

The 69 subjects underwent abdomen MRI on a 3.0 T MR scanner. Seventeen had normal physical examinations, 34 had liver lesions (6 with multiple metastatic liver tumors; 7 with hepatocellular carcinomas confirmed by pathology; 10 with liver cysts; 7 with hepatic hemangiomas; and 4 who simultaneously had liver cysts and hemangiomas), and 18 had fatty livers. The latter patients underwent computed tomography (CT) and/or ultrasonic examinations (US) to confirm the diagnosis.

Table 1 presents the results of the direct comparisons in terms of image quality, fat suppression quality, susceptibility artifacts, and motion artifacts in all subjects. The scores of the quality of the LAVA-Flex water-only images were slightly higher than the FSPGR T1-weighted images, but there were no statistically significant differences ($P > 0.05$). The scores of the fat suppression quality and susceptibility artifacts of the LAVA-Flex water-only images were significantly higher than the FSPGR images according to the five-point-scale qualitative assessment (Figs. 1–3). Although the scores of the motion artifacts were higher in the LAVA-Flex water-only images than the FSPGR T1-weighted images, there was no statistically significant difference ($P = 0.07$) (Fig. 4).

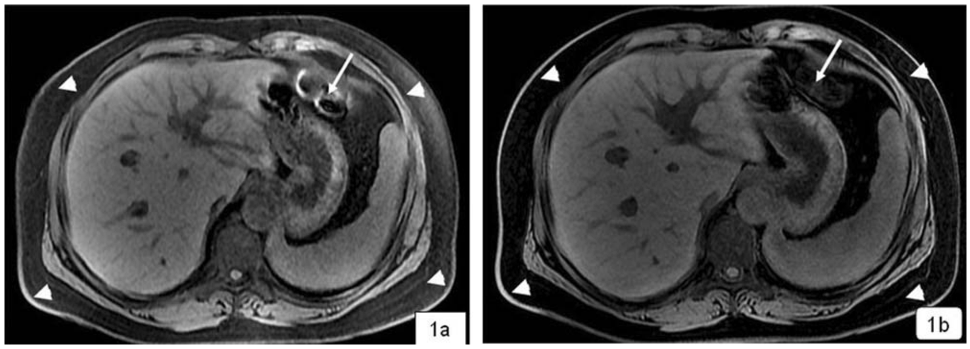

Figure 1. Axial T1-weighted fat-suppressed (**a**) and LAVA-Flex water-only (**b**) MR images of the abdomen show equally good image quality (five points), but both readers judged that the LAVA-Flex water-only image achieved stronger fat suppression (triangle) and fewer susceptibility artifacts (arrow).

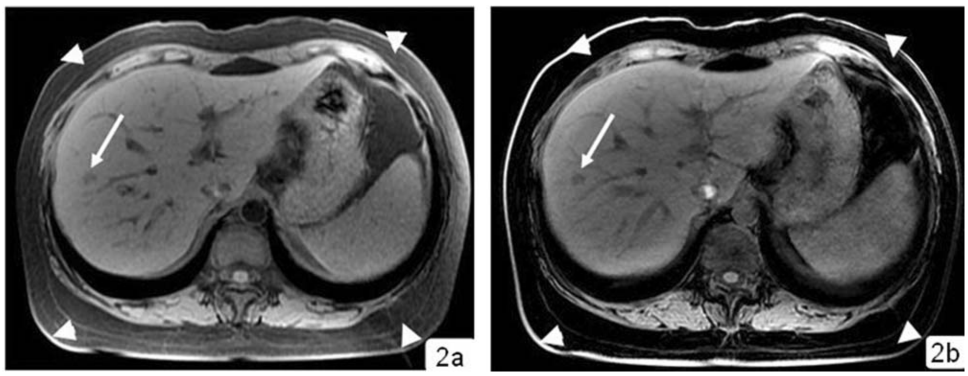

Figure 2. Axial T1-weighted fat-suppressed (**a**) and LAVA-Flex water-only (**b**) MR images of the abdomen show a small lesion (arrow). Both readers judged that the contrast between the normal liver and lesions as well as between the muscle and fat were higher in the LAVA-Flex water-only images and the LAVA-Flex water-only image achieved superior and more homogenous fat suppression (triangle).

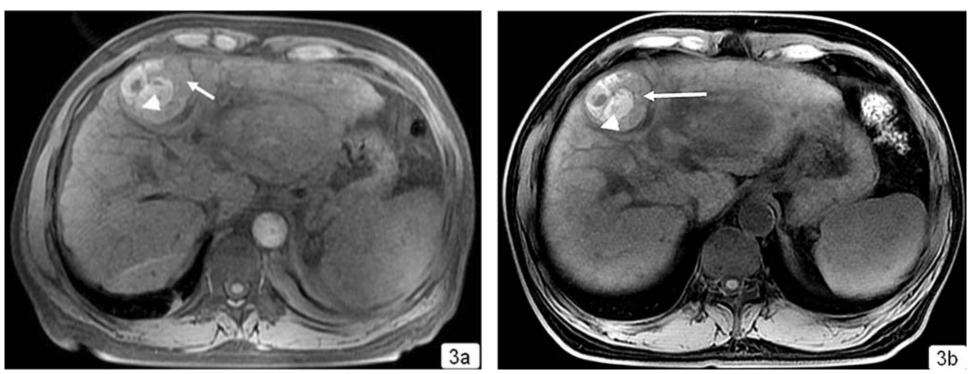

Figure 3. Axial T1-weighted fat-suppressed (**a**) and LAVA-Flex water-only (**b**) MR images of a liver cancer patient's abdomen (arrow). Both readers judged that the visibility of structures within the mass in LAVA-Flex water-only image was more conspicuous (the triangle shows a tumor with hemorrhage).

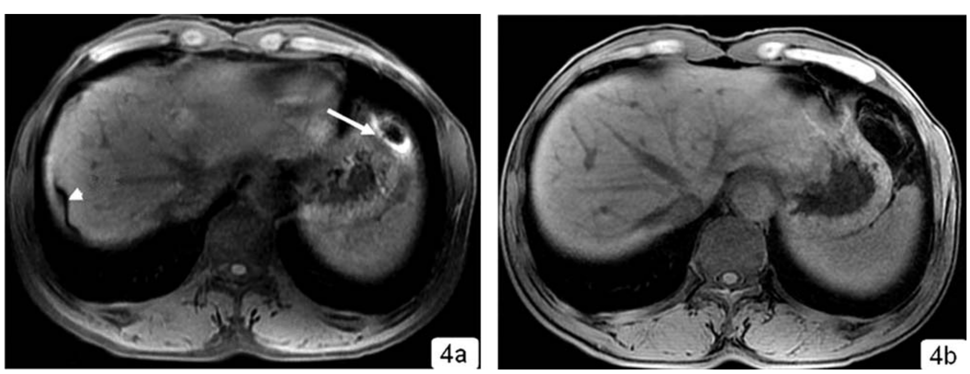

Figure 4. Axial T1-weighted fat-suppressed (**a**) and LAVA-Flex water-only (**b**) MR images of the abdomen show that the T1-weighted fat-suppressed image had more susceptibility artifacts from air in the stomach (arrow). The arrowhead shows the artifact concerning misregistration with calibration acquisition for ASSET.

Table 2
Comparison of the Quantitative Measurements of the Signal Intensity Between the FSPGR T1-Weighted and LAVA-Flex Water-Only Images

Measurement	LAVA-Flex water-only	FSPGR T1-weighted	*P* value
Fat suppression uniformity assessment[a]			
SI of 12 ROIs	417.88 (223.77)	1005.26 (302.85)	0.040
SD of 12 ROIs	62.84 (16.10)	115.13 (36.38)	0.007
SD% f 12 ROIs	4.86(3.15)	7.14(1.79)	0.002
Contrast assessment[a]			
SI_M	2115.56 (348.80)	2252.79 (303.73)	0.407
SI_F	417.88 (223.77)	1005.26 (302.85)	0.040
C_{MF} %	86.28 (5.42)	40.15 (14.4)	0.008
Liver and lesion contrast assessment[b]			
SI_L	1754.12 (302.21)	1438.79 (734.41)	0.023
SI_{LL}	822.30 (487.54)	1217.19 (355.84)	0.242
C_{LLL} %	49.83 (11.22)	45.52 (31.35)	0.043

The data are the mean image quality (standard deviation).
[a]Scores are based on the data obtained from 69 patients.
[b]Scores are based on the data obtained from 39 patients with liver lesions.

Quantitative Assessments

Uniformity of Fat Suppression

The variation in the uniformity of the signal intensity in the FSPGR T1-weighted images (115.13) was significantly higher than that in the LAVA-Flex water-only images (62.84) ($P = 0.007$). The variation in the uniformity of the signal intensity on the water-only dual-echo Dixon images (4.9%) was significantly lower than that on the standard T1-weighted fat-suppressed images (7.1%) ($P = 0.02$) (Table 2).

Contrast Between Muscle and Fat

The SI value of muscle in the FSPGR T1-weighted images (mean value, 2252.79 msec) was higher than that in the LAVA-Flex water-only images (mean value, 2115.79 msec), but there was no statistically significant difference ($P = 0.41$). The image contrast between the muscle and fat was significantly higher in the LAVA-Flex water-only images (mean ratio, 86.28%) than in the FSPGR T1-weighted images (mean ratio, 40.15%) ($P = 0.008$) (Table 2).

Contrast Between the Normal Liver and Liver Lesions

The SI value of normal liver (SI_L) in the LAVA-Flex water-only phase images was higher than in the fat-saturated FSPGR T1WI images ($P = 0.023$). The SI value of the liver lesions (SI_{LL}) was the reverse (822.30 msec vs. 1217.19 msec), but there were no statistically significant differences ($P = 0.242$). The image contrast between the liver and liver lesions (C_{LLL}) was significantly higher in the LAVA-Flex water-only phase images (mean ratio, 49.83%) than in the FSPGR T1-weighted images (mean ratio, 45.52%) ($P = 0.043$) (Table 2).

Contrast Between the Fatty Liver and Spleen in the Fat-Phase Images

The SI of the normal spleen was slightly higher than that of liver on the LAVA-Flex fat-only phase, but the difference was not statistically significant ($P = 0.24$). The SI of the fatty liver was higher than that of the spleen ($P = 0.002$). The value of the C_{FLS} (mean ratio, 54.24%) was higher than that of the C_{LS} (mean ratio, 36.21%) ($P = 0.046$) (Table 3, Figs. 5–7).

DISCUSSION

In this study we found that, compared with FSPGR imaging, LAVA-Flex images had better and more homogenous fat suppression and lower susceptibility artifact. The contrast between muscle and fat and between the liver and pathologic lesions was significantly improved on LAVA-Flex sequence. In addition, we also found the SI of the fatty liver in the LAVA-Flex fat-only phase images was higher than that of the spleen. The value of the C_{FLS} was higher than that of the C_{LS}. LAVA-Flex could offer superior and more homogenous fat suppression of the abdomen and become a routine abdominal sequence protocol for 3.0 T MRI.

LAVA-Flex is a 3D, FSPGR imaging technique that acquires water-only, fat-only, in-phase and out-of-phase echoes in a single acquisition that is typically completed in one 20-second breath-hold (12,13). A key benefit of LAVA Flex is the ability to generate the water-only and fat-only images using preexisting in-phase and out-of-phase raw data without adding scan time. In our study, we found that there were no statistically significant differences in the image quality of the water-only images and the FSPGR T1-weighted images when using the CHESS technique and the five-point-scale qualitative assessment. The reason for this observation is that the two sequences are rooted in FSPGR imaging and only apply two different fat suppression techniques. In our opinion, a more appropriate acquisition sequence for direct

Table 3
Comparison of the Quantitative Measurements of the Signal Intensity Between the Fatty Liver and Spleen in the LAVA-Flex Fat-Phase Images

Parameter	Liver	Spleen	Fatty liver	*P* value
SI value	54.38 (11.70)	67.85 (21.73)		0.239
SI value		182.00 (76.74)	459.78 (251.66)	0.002
Contrast	C_{LS} 36.21 (34.42)		C_{FLS} 54.24 (17.49)	0.046

The data are the mean image quality (standard deviation) based on the data obtained in 18 fatty liver patients.

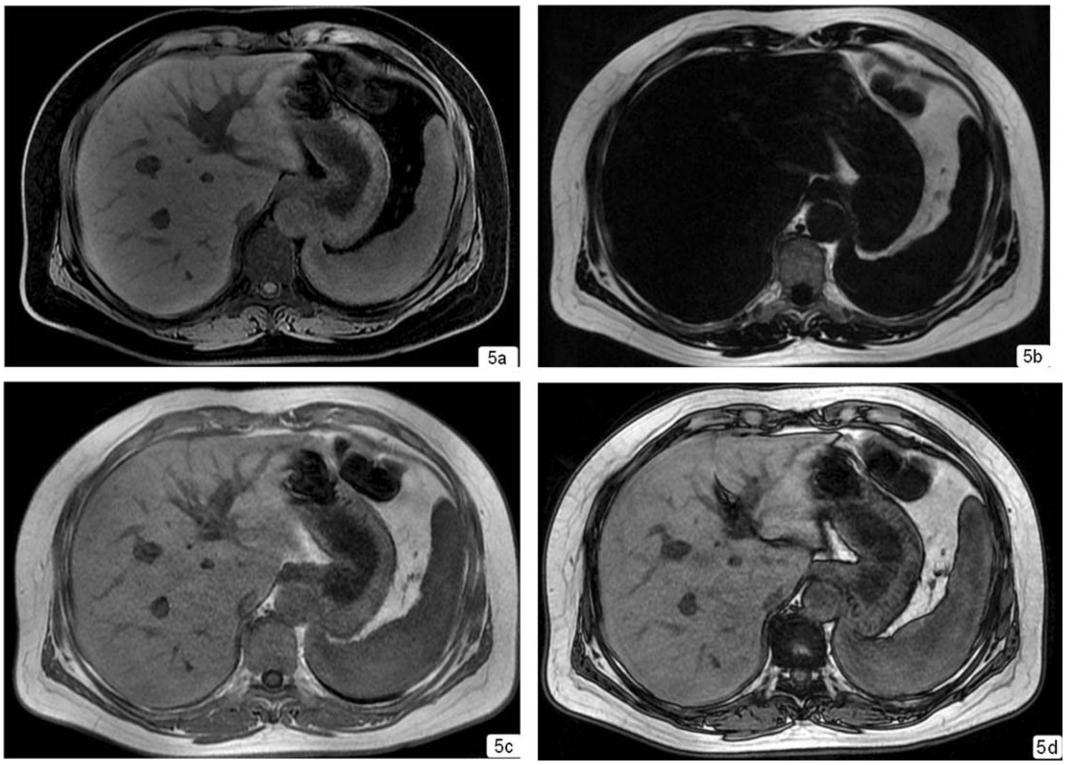

Figure 5. A physical examination case. The water-only (**a**), fat-only (**b**), in-phase (**c**), and out-of-phase (**d**) images on the LAVA-Flex sequence had good image quality.

comparison of fat suppression may have been an equivalent gradient-echo acquisition performed with a conventional CHESS fat suppression method. Moreover, Thoeni et al (24) and Sica et al (25) reported that FSPGR had the advantages of fast scanning and reducing chemical and respiratory artifacts. In

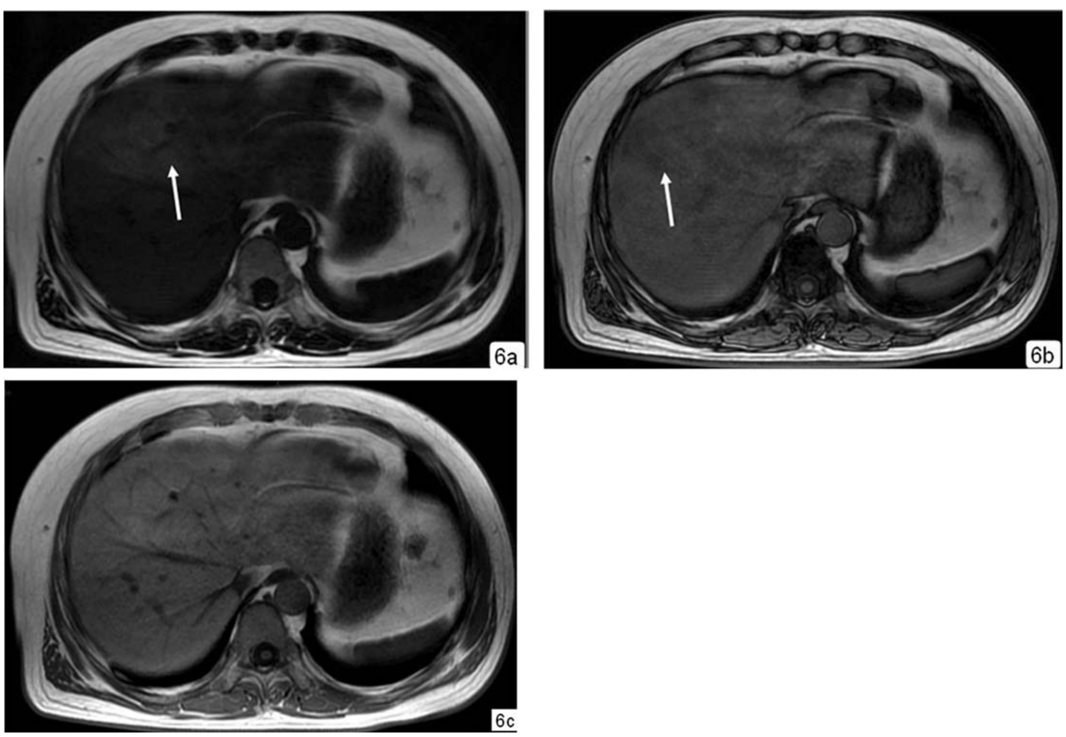

Figure 6. A patient with focal fatty infiltration of the liver. The fat-only image (**a**) showed left lobe liver SI that was obviously higher than that of background noise and spleen (arrow). The out-of-phase T1WI 3D gradient echo image (**b**) demonstrated marked liver signal loss compared to the corresponding in-phase image (**c**).

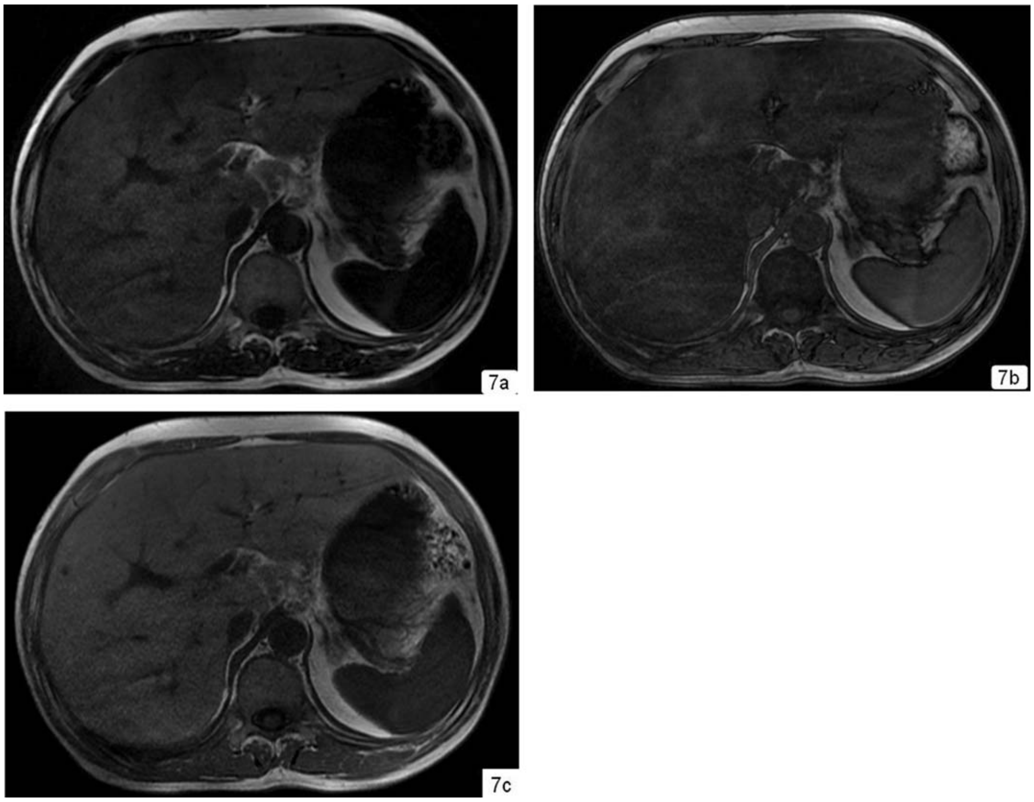

Figure 7. A patient with diffuse fatty infiltration of the liver. The fat-only image (**a**) showed the whole liver SI, which was obviously higher than that of background noise and spleen. The opposed-phase T1WI 3D gradient echo image (**b**) demonstrated that the whole liver signal was markedly lower compared to the corresponding in-phase image (**c**).

addition, both readers subjectively judged the motion artifacts to be equal between the two sequences, presumably because they have the same short acquisition time; time-consuming examinations are often criticized for producing motion artifacts in MRI.

Magnetic resonance techniques provide a noninvasive means of estimating the fat content in vivo (14). Various MRI techniques are used to increase the signal differences and, hence, the depiction of abnormalities by suppressing the high signal intensity of fat (2). Examples of fat-suppression techniques are the STIR, CHESS, CSS-IR, and Dixon methods (7–11).

Fat suppression is useful in the upper abdomen because the motion of high-signal-intensity fat degrades the image quality by inducing phase artifacts (2). The most commonly used fat-suppression technique is the CHESS technique, which is subject to suppression failures because it assumes that the absolute precession frequencies of fat and water are constant and known precisely over the entire imaging volume (26). The T1-weighted FSPGR sequence described in our study applied a CHESS technique that is sensitive to constant magnetic induction field and radiofrequency magnetic induction field inhomogeneities, which may cause inadvertent water suppression, substantially reducing the signal-to-noise ratio (SNR) of the image (4,26). Dixon techniques, in contrast, exploit the relative precession frequency between fat and water to eliminate the fat signal and may provide a useful alternative means of better and more uniform fat suppression (4,26).

The results of our study demonstrate that the fat suppression applied two-point Dixon technique yields higher quality and more uniform fat suppression water-only images. With this sequence, the contrast between muscle and fat was significantly greater than in standard FSPGR T1-weighted CHESS fat-suppressed imaging, as was the contrast between the normal liver and lesions. In addition, both readers subjectively judged the susceptibility artifacts to be significantly lower with the Dixon technique because this technique is insensitive to the B0 inhomogeneities and leads to better and more uniform fat suppression (4,26).

A dual-echo Dixon technique has been used to image various anatomic sites and yielded encouraging results. Beddy et al (4) concluded that dual-echo Dixon imaging facilitates improved image quality of fat-suppressed images of the pelvis compared with standard T1-weighted fat-suppressed imaging, thus enabling better delineation of pathologic lesions. Cornfeld et al (27) also found that the dual-echo two-point Dixon sequence achieved stronger fat suppression in the female pelvis when compared with 3D FSPGR sequences with spectral inversion at the lipids. Ragan and Bankson (26) found that Dixon fat separation provides more reliable and homogenous fat suppression than chemical saturation in phantoms and in vivo. Our results were similar to those reported by the aforementioned investigators (4,26,27).

Over the last two decades, the increased prevalence of being overweight or obese most likely explains the emergence of fatty liver disease (28), which affects 10%

to 30% of adults (29,30) and 13% of children (31) in the general population. Thus, liver fat quantification has generated considerable interest and may be of clinical importance for reliably measuring the liver fat content (FC). There is currently no specific biochemical or quantification test for fatty liver (28). Liver biopsy and histological analysis are considered the diagnostic reference standard (32). However, the biopsy procedure is invasive and cannot be performed repeatedly to measure fat changes following treatment; in addition, it presents risks for patients (33). MRI techniques provide a noninvasive means of estimating and quantifying the fat content (14,34). Proton magnetic resonance spectroscopy (MRS) is currently considered the most accurate noninvasive technique for detecting fat levels. However, MRS is too time-consuming for routine clinical practice and requires a skilled operator to correctly perform the examination, process the data, and interpret the results (28). Westphalen et al (35) and Schuchmann et al (36) stated that the original two-point Dixon method in conjunction with a spoiled gradient echo sequence (SPGR) is often used in the quantification of the hepatic fat fraction due to its simplicity. In our study, we found the SI of fatty liver with the LAVA-Flex fat-only phase was higher than that of the spleen and the value of the C_{FLS} was also higher than the C_LS. This may mean that diffuse and focal liver fat was displayed well and quantified noninvasively for the fat-only phase in the LAVA-Flex images.

One limitation of this study was its retrospective nature. Additionally, the LAVA-Flex technique was not compared with other fat-attenuating sequences. However, the standard T1-weighted FSPGR CHESS fat-suppression technique was used to evaluate the abdominal examinations at our institution. Another limitation is that pathologic proof was not available for all patients. However, the patient history, imaging characteristics, biopsy results, and surgery findings were used as diagnostic criteria; furthermore, the liver fat cases were confirmed by CT and/or US. In addition, we simply studied the performance of the liver fat with fat-only phase imaging because the chief objective of our study was to compare the water-only phase of the LAVA-Flex sequence with the T1-weighted FSPGR sequence using the CHESS technique. Therefore, these limitations most likely do not impact the accuracy and significance of our results.

In conclusion, compared with the standard T1-weighted FSPGR sequence using the CHESS technique, the 3D LAVA-Flex sequence offers superior and more homogenous fat suppression of the abdomen. Fat-only phase images may be a simple and effective method for helping predict clinical assessment of fatty liver. LAVA-Flex could become a routine abdominal sequence protocol in 3.0 T MRI.

REFERENCES

1. Lu DS, Saini S, Hahn PF, et al. T2-weighted MR imaging of the upper part of the abdomen: should fat suppression be used routinely? AJR Am J Roentgenol 1994;162:1095–1100.
2. Semelka RC, Chew W, Hricak H, et al. Fat-saturation MR imaging of the upper abdomen. AJR Am J Roentgenol 1990;155:1111–1116.
3. Chan TW, Listerud J, Kressel HY. Combined chemical-shift and phase-selective imaging for fat suppression: theory and initial clinical experience. Radiology 1991;181:41–47.
4. Beddy P, Rangarajan RD, Kataoka M, et al. T1-weighted fat-suppressed imaging of the pelvis with a dual-echo Dixon technique: initial clinical experience. Radiology 2011;258:583–589.
5. Kier R, Smith RC, Mccarthy SM. Value of lipid- and water-suppression MR images in distinguishing between blood and lipid within ovarian masses. AJR Am J Roentgenol 1992;158:321–325.
6. Rofsky NM, Lee VS, Laub G, et al. Abdominal MR imaging with a volumetric interpolated breath-hold examination. Radiology 1999; 212:876–884.
7. Bley TA, Wieben O, Francois CJ, et al. Fat and water magnetic resonance imaging. J Magn Reson Imaging 2010;31:4–18.
8. Dixon WT. Simple proton spectroscopic imaging. Radiology 1984; 153:189–194.
9. Foo TK, Sawyer AM, Faulkner WH, et al. Inversion in the steady state: contrast optimization and reduced imaging time with fast three-dimensional inversion-recovery-prepared GRE pulse sequences. Radiology 1994;191:85–90.
10. Mito S, Ishizaka K, Nakanishi M, et al. Comparison of fat suppression techniques of bilateral breast dynamic sequence at 3.0 T: utility of three-point DIXON technique. Nihon Hoshasen Gijutsu Gakkai Zasshi 2011;67:654–660.
11. Ishizaka K, Oyama N, Mito S, et al. Comparison of 1H MR spectroscopy, 3-point DIXON, and multi-echo gradient echo for measuring hepatic fat fraction. Magn Reson Med Sci 2011;10:41–48.
12. Ma J. Dixon techniques for water and fat imaging. J Magn Reson Imaging 2008;28:543–558.
13. Ma J. Breath-hold water and fat imaging using a dual-echo two-point Dixon technique with an efficient and robust phase-correction algorithm. Magn Reson Med 2004;52:415–419.
14. Kim H, Taksali SE, Dufour S, et al. Comparative MR study of hepatic fat quantification using single-voxel proton spectroscopy, two-point dixon and three-point IDEAL. Magn Reson Med 2008; 59:521–527.
15. Hori M, Kim T, Onishi H, et al. Ovarian masses: MR imaging with T1-weighted 3-dimensional gradient-echo IDEAL water-fat separation sequence at 3T. Magn Reson Med Sci 2012;11:117–127.
16. Cha JG, Jin W, Lee MH, et al. Reducing metallic artifacts in post-operative spinal imaging: usefulness of IDEAL contrast-enhanced T1- and T2-weighted MR imaging—phantom and clinical studies. Radiology 2011;259:885–893.
17. Murakami M, Mori H, Kunimatsu A, et al. Postsurgical spinal magnetic resonance imaging with iterative decomposition of water and fat with echo asymmetry and least-squares estimation. J Comput Assist Tomogr 2011;35:16–20.
18. Chen CA, Lu W, John CT, et al. Multiecho IDEAL gradient-echo water-fat separation for rapid assessment of cartilage volume at 1.5 T: initial experience. Radiology 2009;252:561–567.
19. Grayev A, Shimakawa A, Cousins J, et al. Improved time-of-flight magnetic resonance angiography with IDEAL water-fat separation. J Magn Reson Imaging 2009;29:1367–1374.
20. Costa DN, Pedrosa I, Mckenzie C, et al. Body MRI using IDEAL. AJR Am J Roentgenol 2008;190:1076–1084.
21. Reeder SB, Pineda AR, Wen Z, et al. Iterative decomposition of water and fat with echo asymmetry and least-squares estimation (IDEAL): application with fast spin-echo imaging. Magn Reson Med 2005;54:636–644.
22. Xia Y, Zheng S. Reversed laminar appearance of articular cartilage by T1-weighting in 3D fat-suppressed spoiled gradient recalled echo (SPGR) imaging. J Magn Reson Imaging 2010;32:733–737.
23. Kataoka M, Kido A, Koyama T, et al. MRI of the female pelvis at 3T compared to 1.5T: evaluation on high-resolution T2-weighted and HASTE images. J Magn Reson Imaging 2007;25:527–534.
24. Thoeni RF, Mueller-Lisse UG, Chan R, et al. Detection of small, functional islet cell tumors in the pancreas: selection of MR imaging sequences for optimal sensitivity. Radiology 2000;214:483–490.
25. Sica GT, Miller FH, Rodriguez G, et al. Magnetic resonance imaging in patients with pancreatitis: evaluation of signal intensity and enhancement changes. J Magn Reson Imaging 2002;15:275–284.
26. Ragan DK, Bankson JA. Two-point Dixon technique provides robust fat suppression for multi-mouse imaging. J Magn Reson Imaging 2010;31:510–514.

27. Cornfeld DM, Israel G, McCarthy SM, et al. Pelvic imaging using a T1W fat-suppressed three-dimensional dual echo Dixon technique at 3T. J Magn Reson Imaging 2008;28:121–127.
28. Pacifico L, Martino MD, Catalano C, et al. T1-weighted dual-echo MRI for fat quantification in pediatric nonalcoholic fatty liver disease. World J Gastroenterol 2011;17:3012–3019.
29. Wieckowska A, Mccullough AJ, Feldstein AE. Noninvasive diagnosis and monitoring of nonalcoholic steatohepatitis: present and future. Hepatology 2007;46:582–589.
30. Gastaldelli A, Cusi K, Pettiti M, et al. Relationship between hepaticisceral fat and hepatic insulin resistance in nondiabetic and type 2 diabetic subjects. Gastroenterology 2007;133:496–506.
31. Schwimmer JB, Deutsch R, Kahen T, et al. Prevalence of fatty liver in children and adolescents. Pediatrics 2006;118:1388–1393.
32. Peng XG, Ju S, Qin Y, et al. Quantification of liver fat in mice: comparing dual-echo Dixon imaging, chemical shift imaging, and 1H-MR spectroscopy. J Lipid Res 2011;52:1847–1855.
33. Joy D, Thava VR, Scott BB. Diagnosis of fatty liver disease: is biopsy necessary? Eur J Gastroenterol Hepatol 2003;15:539–543.
34. Lee SS, Park SH, Kim HJ, et al. Non-invasive assessment of hepatic steatosis: prospective comparison of the accuracy of imaging examinations. J Hepatol 2010;52:579–585.
35. Westphalen AC, Qayyum A, Yeh BM, et al. Liver fat: effect of hepatic iron deposition on evaluation with opposed-phase MR imaging. Radiology 2007;242:450–455.
36. Schuchmann S, Weigel C, Albrecht L, et al. Non-invasive quantification of hepatic fat fraction by fast 1.0, 1.5 and 3.0 T MR imaging. Eur J Radiol 2007;62:416–422.